An Experimental and Numerical Study on the Bearing Capacity of Circular and Ring Footings on Rehabilitated Sand Slopes with Geogrid

N. Hataf[1*] and A. Fatolahzadeh[2]

1. Prof. Department of Civil and Environmental Engineering, Shiraz University, Shiraz, Iran
2. M.Sc. graduated, Department of Civil and Environmental Engineering, Shiraz University, Shiraz, Iran

Corresponding author: *nhataf@shirazu.ac.ir*

ARTICLE INFO

ABSTRACT

This paper presents the results of a series of small-scale model tests and numerical analyses conducted on circular and ring model footings located near geogrid reinforced sand slopes. Layers of geogrid were applied as reinforcement. For numerical analyses Finite Element Method (FEM) was used. The effects of reinforcement depth, size, number of layers, and the horizontal distance between reinforcement and the slope surface were experimentally inspected. Moreover, the effects of other parameters such as slope angle, the distance of the footing from the slope crest (for circular footings) and the ratio of inner to outer diameters (for ring fittings) were also numerically inspected. The results of numerical analyses were compared with the laboratory test results and found to be in fair agreement. Optimum bearing capacity values were found for some studied parameters. The results indicate that if the reinforcement layers are implemented correctly, the bearing capacity of circular and ring footings over slopes would significantly increase.

1. Introduction

There are many occasions where shallow foundations are built near natural or man-made soil slopes. In these cases, the bearing capacity may decrease compared to that of the same footing on a horizontal ground surface. Various techniques such as Soil improvement or reinforcement technics can be employed in these cases to increase the bearing capacity.

During recent decades, soil reinforcement as a method of bearing capacity improvement has gained the attention of many geotechnical engineering specialists. Geosynthetics, which are nowadays widely used, are the most popular category. This term refers to a family of products varied in

physical and mechanical properties, having several applications such as environmental, geotechnical and agricultural engineering. Among geosynthetics, geogrids are mainly applied to ameliorate the bearing capacity of soils under shallow foundations and to stabilize soil slopes.

The idea of soil reinforcement dates back to centuries ago when the romans used natural fibers to improve roads on unstable soil. The first laboratory examinations on soil reinforcements were conducted in the 1970s applying metal rods and strips as reinforcement layers [1].

Investigations on the bearing capacity of shallow footings on reinforced soil has been the subject of numerous studies. Circular and ring footings are commonly applied as the foundations of storage tanks and chimneys; some may be located near slopes. There have been a few research studies on the bearing capacity of circular and ring footings on reinforced soil [2, 3]; However, all of them were conducted on horizontal soil surfaces.

Although some studies have been conducted on the bearing capacity of shallow footings located near reinforced slopes, these studies were limited to strip footings, assuming the plain-strain condition [4-7]. On the other hand, circular and ring footings have been inspected on horizontal soil surfaces and some unique behaviors are found for them [8]; Hence, further research was acquired to explore these foundations near slopes and in particular, reinforced slopes. The main purpose of this study is to the effect of reinforcement of sand slopes (using geogrid layers) on the bearing capacity of circular and ring footings situated near them. In order to fulfill this aim, an experimental approach was adopted and a series of loading tests

were conducted. Several numerical models were also made and their results were validated by those of experimental test. In addition, the effect of some other parameters was investigated applying numerical simulations as well.

2. Laboratory Investigations

The geometrical parameters of a typical geogrid reinforced slope are indicated in Fig. 1. The variable parameters of the geogrid layers which were intended for experimental investigation are: first reinforcement layer depth (u), length of reinforcement layer (l), width of reinforcement layer (b), distance of the reinforcement layer from the slope surface (x), and the number of layers (N). It is noteworthy to mention that the length and the width of layers were assumed equal and layer spacing (h) was kept constant during the examinations.
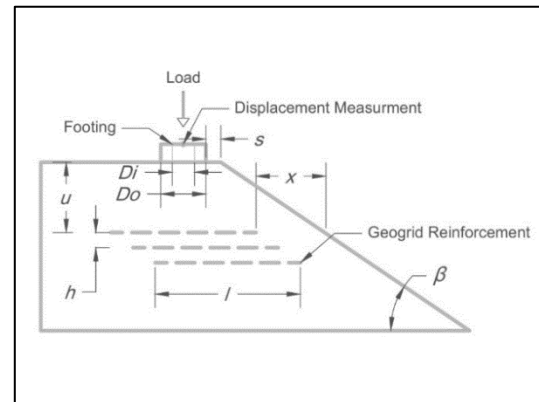

Fig. 1. Parameters investigated by experimental tests.

In order to inspect the aforementioned parameters, a series of tests were outlined and conducted in the laboratory. Denomination of these tests, constants and variables are portrayed in Table1. Test arrangements were selected in such a way that all but one parameter were identical in each set. Therefore, by comparing the

obtained values of bearing capacity for a set of tests, the effect of variation in each parameter could be separately investigated. In the present study, tests were conducted on two small scale circular and ring model footings made from stiff Teflon polymer. For all tests, the circular model footing had the diameter of 15cm while the ring foundation had the outer (Dout) and the inner (Din) diameters of 15cm and 6cm, respectively (i.e., Din/Dout=0.4), as applied by [3]. The distance between the footing and the slope crest (s) was 5cm and the slope angle (β) of 34˚ (1(H):0.67(V)) were constant in all laboratory tests.

2.1 Test Apparatus

The model tests were carried out in a stiff box having the dimensions of 185×80×80cm made from glass and steel sheets and braced using steel profiles. The dimensions of the box were selected in the light of a preliminary numerical sensitivity analysis to avoid boundary effects. A rigid steel frame was installed over the box to keep the loading apparatus in place. The box and frame are presented in Fig. 2.

Fig. 2. Test box and loading apparatus.

2.2 Material Tested

The sand used in this study was well-graded and sub-angular. It was washed before being used to eliminate the fine particles and to remove cohesion. It was then spread thinly and allowed to dry for weeks. The water content was frequently measured until the results were all below 0.3%. Consequently, the sand could be contemplated dry. Additionally, the sieve test was conducted to obtain the grain size distribution. Some physical properties of the sand are reported in Table 2.

Table 1. Denomination of experimental tests and their corresponding properties.

Test ID	Footing Type	N	u (cm)	l*l (cm)	x (cm)
CU00	Circ.	-	-	-	-
CR01	Circ.	1	5	30*30	0
CR02	Circ.	1	5	45*45	0
CR03	Circ.	1	5	60*60	0
CR04	Circ.	1	7.5	45*45	0
CR05	Circ.	1	10	45*45	0
CR06	Circ.	1	15	45*45	0
CR07	Circ.	1	20	45*45	0
CR08	Circ.	1	10	45*45	5
CR09	Circ.	1	10	45*45	10
CR10	Circ.	2	5	45*45	0
CR11	Circ.	3	5	45*45	0
RU00	Ring	-	-	-	-
RR01	Ring	1	5	30*30	0
RR02	Ring	1	5	45*45	0
RR03	Ring	1	5	60*60	0
RR04	Ring	1	7.5	45*45	0
RR05	Ring	1	10	45*45	0
RR06	Ring	1	15	45*45	0
RR07	Ring	1	20	45*45	0
RR08	Ring	1	10	45*45	5
RR09	Ring	1	10	45*45	10
RR10	Ring	2	5	45*45	0
RR11	Ring	3	5	45*45	0

In order to build the sand slope, the box was filled and compacted in 10cm layers. Furthermore, the desired position of sand slope was marked inside the box to control

the slope surface accurately. A steel plate of 40cm×40cm×5mm and the mass of 6.5Kg was dropped from 20cm height to compact the layers. To ensure that the soil was compacted horizontally uniform, the plate was dropped 10 times on each point. After the soil body had reached the desired height (80cm), it was cut to the slope surface, conforming to the markers on the test box. The cutting process was done so precise that the final slope surface remained undisturbed as much as possible.

Table 2. Physical properties of the sand

γ	19.8 kN/m^3
D_{10}	0.06 mm
D_{30}	0.45 mm
D_{60}	2 mm
C_u	28.5
C_c	1.45
Classification	SW
Water Content	< 0.3%

2.3 Reinforcements

In this study, the tested geogrid was of CE131 model, which was applied in previous studies [4, 6]. The detailed specifications of this geogrud is presented in Table 3.

Table 3. CE131 geogrid specifications.

Polymer type	HDPE
Mesh aperture	27×27 mm
Mesh thickness	5.2 mm
Mass per unit area	660 gr/m^2
Max. tensile strength	28 kN/m
Max. tensile force	5.8 kN

3. Testing Procedure

Before each test, the slope was built using the mentioned procedure in advance. The footing and displacement gauges were then put in place. An initial load was applied before zeroing the displacement gauges to make the footing firmly fit on the soil surface. This provided an appropriate start point for displacement measurement and made the loading curves comparable. Consequently the load was applied in steps while the corresponding displacements of each step were recorded. The interval between load steps was 20 min to allow the displacements to become stable. The loading was continued until the slope collapsed or until the full extension of load jack (5 cm).

4. General Observations

During the final stages of most tests, different failure patterns could be observed. However, they were not distinguishable in all tests. Generally, when the slope was unreinforced or the reinforcement layers were implemented relatively deep, harsh local slope instabilities occurred and the footing rotated strongly towards the slope face, presented in Fig. 3. On the other hand, when the reinforced layers were shallow or several layers were implemented, the punching mechanism was prevalent.

Fig. 3. Failure mode of ring footing

5. Experimental Results

The applied loads and their corresponding displacements were plotted for each test to

acquire a load-displacement curve. The curves were consequently plotted together in different groups so that in each group, the effect of just one parameter of geogrid reinforcement could be Inspected. For instance, the load-displacement curves which describe the effect of reinforcement depth are plotted in Fig. 4a and Fig. 4b for circular and ring model footings, respectively. Although the effect of this parameter is evident, it cannot be directly quantified; Therefore, it is necessary to compute the ultimate bearing capacity of each test in order to make the data comparable.

The bearing capacity of a footing can be determined from load-displacement curves in many ways. The "tangent intersection method" was applied in this study [9]. In this procedure, as illustrated in Fig. 5, the corresponding load in the intersection point of the tangents of the start and the end parts of the load-displacement curve is assumed to represent the ultimate bearing capacity.

Since this study deals with geogrid layers of reinforcement, a non-dimensional factor, known as "Bearing Capacity Ratio (BCR)", was used to facilitate the investigation. This factor is defined as the ratio of the ultimate bearing capacity of a footing rested on the reinforced soil to the comparable value of ultimate bearing capacity in the unreinforced case.

Thus, in order to explore the effects of reinforcement layers on the bearing capacity of a footing, values of BCR were plotted. It is noteworthy to mention that the parameters of reinforcement in this study are presented in a non-dimensional form in order to make them comparable to the results of other studies which were conducted on footings of different shapes and dimensions. In this

regard, the parameters of reinforcement depth, size, distance from slope surface and the number of reinforcement layers (defined in Fig. 1) are presented as u/D, l/D, x/D and N, respectively.
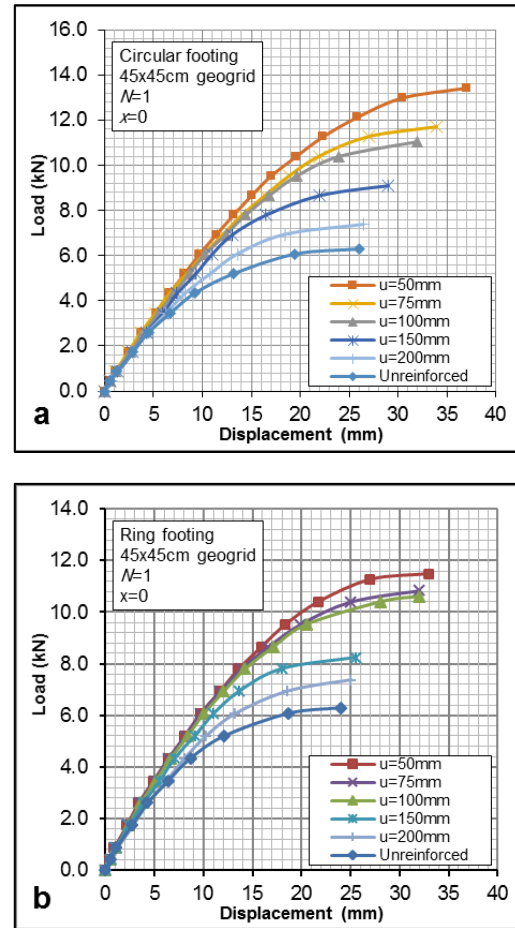

Fig. 4. Load-displacement curves as a function of reinforcement depth for: a) Circular footing, b) Ring footing.
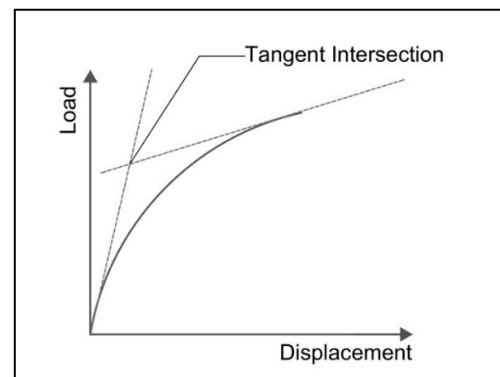

Fig. 5. Tangent intersection method for evaluation of ultimate bearing capacity.

5.1 Effect of Reinforcement Depth

Fig. 6 indicates the effect of reinforcement depth on the bearing capacity of circular and ring model footings. The values of BCR are acquired for depths of u/D=0.3, 0.6, 1.0, 1.5 and 2.0. As is evident, the trend is similar for both circular and ring model footings in which the maximum of BCR occurs when u/D=0.3. This outcome is consistent with the results of previous studies on the strip or square footings [10, 11] as almost all of them have suggested that the maximum of BCR happens when the reinforcement depth is minimum.
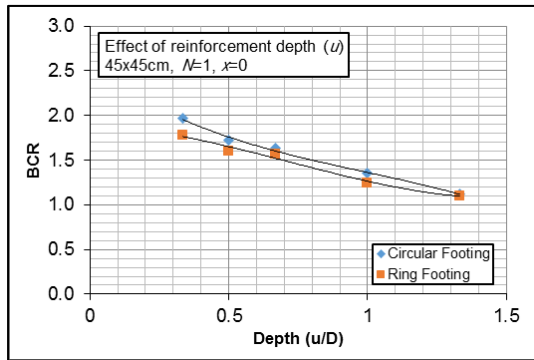
Fig. 6. Effect of reinforcement depth on BCR.

It can also be inferred that if the geogrid layers are implemented deeper than u/D=1.25, the effect of reinforcement on bearing capacity of the footing is negligible. On that account, u/D=1.25 can be called "the zone of influence of reinforcement".

5-2 Effect of Reinforcement Size

In Fig. 7, the BCR values are given for slopes reinforced with square layers of 30×30, 45×45 and 60×60cm which can be represented as l/D=2.0, 3.0 and 4.0, respectively. It can be observed that the BCR increases with layer size and the maximum occurs when l/D=4.0. However, for sand slopes reinforced with geogrid layers of l/D=3.0 and larger, the BCR does not change

significantly; Hence, the l/D=3.0 can be defined as "the maximum effective size".

Previous studies suggest different values for optimum reinforcement size depending on various footing type and reinforcement configuration they applied[10, 12, 13].
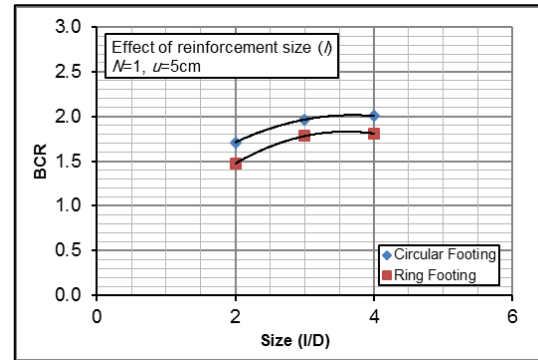

Fig. 7. Effect of reinforcement size on BCR.

5-3 Effect of Distance of Reinforcement from Slope Surface

Fig. 8 reveals the results of model tests conducted on sand slopes reinforced with geogrid layers having distances of x/D=0, 0.5, 1.0 and 1.5. It can be seen that when the geogrid layer is right beside slope surface (x/D=0), the BCR is maximum. This observation is in accordance with the findings of previous studies on strip footings [14].

As the distance of reinforcement layers from slope surface increases, The BCR drops significantly so that for x/D values greater than 2.0, the effect of reinforcement is negligible. Thus, the x/D=2.0 can be contemplated as the "the distance of influence".

5.4 Effect of Number of Reinforcement Layers

The variation of BCR versus the number of reinforcement layers is presentedin Fig. 9. It is evident that BCR rises as the number of

geogrid layers increases. Although the trend is still increasing for N=3 and no optimum value is acquired, considering the zone of influence of reinforcement, the risk of confinement effects and feasibility in practical applications, no further tests were carried out for higher numbers of reinforcement layers.
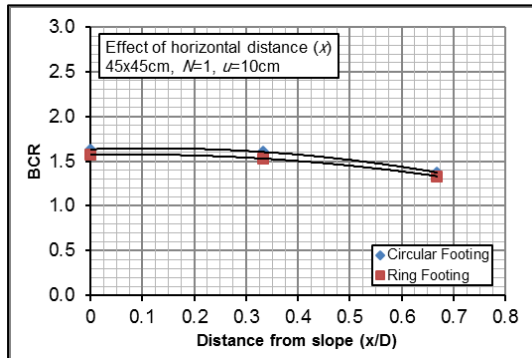

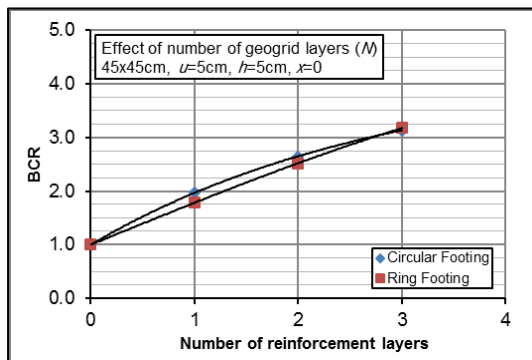**Fig. 8.** Effect of distance between reinforcement and the slope surface.

Fig. 9. Effect of number of geogrid layers on BCR.

5.5 Comparison of Circular and Ring Footings

As can be observed in Fig. 4a and Fig. 4b, the trend and the ultimate loads are almost identical for both circular and ring model footings. This is in accordance with the findings of [3, 8] which suggest that the ultimate bearing capacity and BCR of ring footings with the ring ratio less than 0.4 ($D_{in}/D_{out}<0.4$) is the same as those of circular footings. However, in contrast with

the aforementioned studies which are performed on the horizontal ground, the present study deals with sand slopes and the optimum limit of ring ratio should be explored again. As described later, this evaluation is performed by numerical analysis and it was computed that the optimum ring ratio for footings located on sand slopes is 0.4, similar to horizontal surface cases.

By a cursory glance at the results depicted in Figs 6-9, it can be stated that although the effect of the parameters reveals a similar trend for both circular and ring model footings, the values of BCR were slightly higher for circular types. In other words, the implementation of reinforcement layers in a sand slope was more efficient in the case where the footing near the slope is circular.

6. Numerical Modeling

The accuracy of the results acquired from small-scale models is limited. Moreover, it may not be feasible to control the values of some parameters, e.g., the slope angle applying laboratory tests since cutting the slope to a mild angle is difficult to attain. Furthermore, when the effect of one parameter is going to be inspected, keeping all other parameters constant is not totally achievable and models may vary in terms of compaction inhomogeneity and segregation of particles. Numerical simulation is indicated to be effective for overcoming these difficulties. Besides, by applying verified and calibrated numerical simulations, additional parameters can be investigated as well. In this study, Plaxis 3D software which is based on the finite element method (FEM) was used to conduct preliminary sensitivity analyses and also to

investigate the effects of the remaining parameters.

6.1 Numerical Simulation Workflow

In order to inspect the effect of the remaining parameters, the FEM software was verified first. Two tests (CU00 and CR02) which represented both unreinforced and reinforced cases were simulated by the software. The mechanical properties of sand mentioned by [3] were verified by performing further direct shear tests and were applied in the numerical simulations. These properties are presented in Table 4. The numerically obtained load-displacement curves were compared to the experimental results, illustrated in Fig. 10. It can be observed that the numerical results conform to the experimental ones in both unreinforced and reinforced cases. This gave the confidence that the software could be applied to examine the effect of other parameters on bearing capacity of the footings. These parameters include the slope angle (β), the distance between the footing and the slope (s) and the ring ratio (Din/Dout) (defined in Fig. 1).

The simulation workflow was straightforward and similar in all models. First, the geometry of the model was defined and the material properties were assigned to the soil and the geogrid layer (if existed in the test) was implemented. Fig. 11 illustrates the sand slope after it was defined in the FEM software.

The Mohr-Coulomb failure criterion was selected for the sand slope due to the the available parameters from the direct shear test.
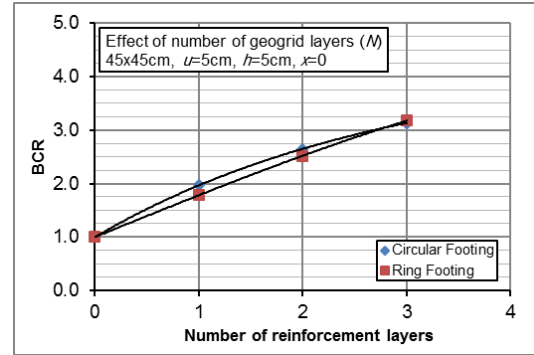

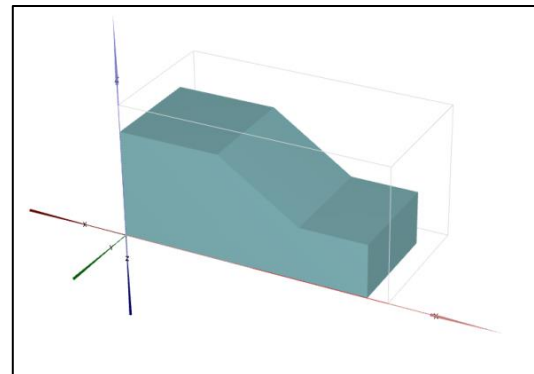**Fig. 10.** Comparison of experimental and numerical results.

Fig. 11. The geometry of the sand slope defined in the FEM software.

The geogrid behavior was assumed elastoplastic contemplating the properties introduced before. It is noteworthy to mention that Plaxis models the geogrid as a tensile-only planar element which its interaction with the adjacent soil is defined by interfaces. The shear strength of interface elements is defined as a fraction of the strength of the nearby soil. In order to the fact that this study dealt with slopes, the gravity method was applied to evaluate the initial stresses. The footing was assumed stiff and the prescribed displacement was imposed on its center line to allow for possible rotations.

The Plaxis software could not directly calculate the bearing capacity; Hence, a prescribed displacement was applied to the footing incrementally while its reaction force

was logged for each step. Consequently, the load-displacement curve was plotted. The procedure for calculation of the bearing capacity is the same as that for the experimental test results, i.e. applying the tangent intersection method discussed above.

Table 4. Soil parameters used in numerical simulations.

|	
γ	19.8 kN/m^3
E	8000 kN/m^2
φ	38°
C	3 kN/m^2

6.2 Sensitivity Analysis

First, mesh sensitivity analysis was performed to optimize meshes applied in finite element modeling. The results are depicted in Fig. 12-a. The load-displacement curves are given for three similar models with the coarsest, the finest and the selected optimized mesh. Clearly, the difference between the results of the finest mesh and the selected one is insignificant. An optimized mesh size used in the sensitivity analyses is presented in Fig. 12-b.

A series of finite element simulations were consequently conducted to assure the results are independent of the boundary conditions of the sand slope. If the boundary conditions were too close to the footing, confinement may have been occurred, affecting the bearing capacity.

As Fig. 13 exhibits, when defining models with similar soil properties and footing dimensions, the load-displacement curves of the footings did not change with box size. On that account, the boundary effects on the results of model tests conducted within the box were negligible. However, because of the fact that the further numerical investigation of the distance of the footing from the slope (s) needs more soil body, expanded

boundaries were applied in further simulations.
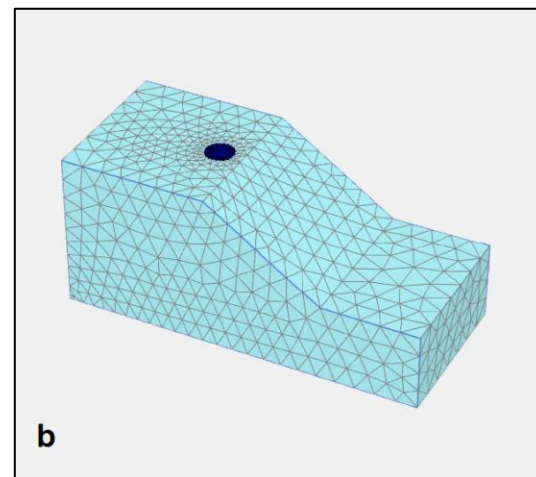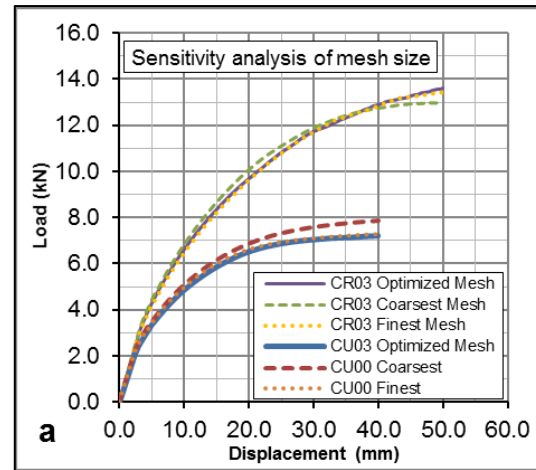
Fig. 12. a) Sensitivity analysis of mesh size, b) The optimized mesh used in simulations.
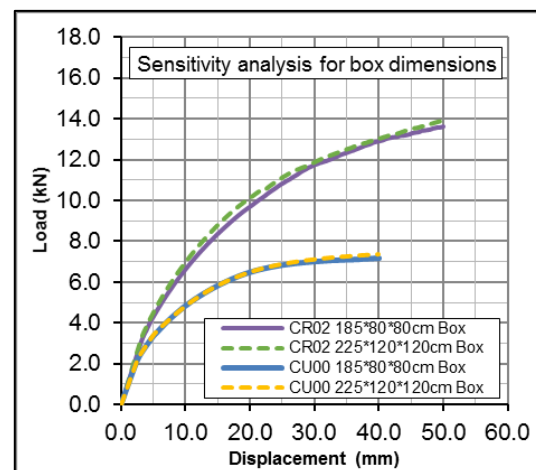
Fig. 13. Sensitivity analysis of box size (boundaries).

7. Numerical Results

7.1 Effect of Slope Angle

A number of models were numerically simulated to study the effect of the angle of the sand slope on the bearing capacity of the footings. The load-displacement curves of 14 models, with slope angle (β) ranging between zero (horizontal ground) and 45˚, are plotted in Fig. 14-a and b for unreinforced and reinforced sand slopes. In order to make the data comparable, applying the tangent intersection method, the load bearing capacities values versus their corresponding values of slope angle are plotted in Fig. 15. It can be noticed that, as the angle of sand slope increases, bearing capacity of the footing falls significantly for both unreinforced and reinforced cases. For instance, the bearing capacity of the circular footing on a 45˚ unreinforced slope is 40% less than the horizontal ground.

7.2 Effect of Distance of Footing from Slope

As previous studies indicate, the distance of the footing from slope crest affects the bearing capacity of nearby strip footings [14] (El Sawwaf 2007). This effect was examined for circular foundations applying numerical analysis. 16 models, with a slope angle of β=34˚ and a ratio of distance to footing diameter (s/D) varying between 0.3 and 4.0, were defined in both unreinforced and reinforced cases. The resulting load bearing capacities of these models are portrayed in Fig. 16.

It is evident that the bearing capacity increases as the footing is moved away from the slope crest. However, its rate declines to the extent that it doesn't change for s/D values greater than 3.0. This can be

contemplated alongside the results reported by [14, 4].Despite to that, it should be noticed that the slope influence distance is obtained for β=34˚ and seems to be dependent on the slope angle as and the soil parameters. As a result, further experiments or simulations should be made for practical purposes.
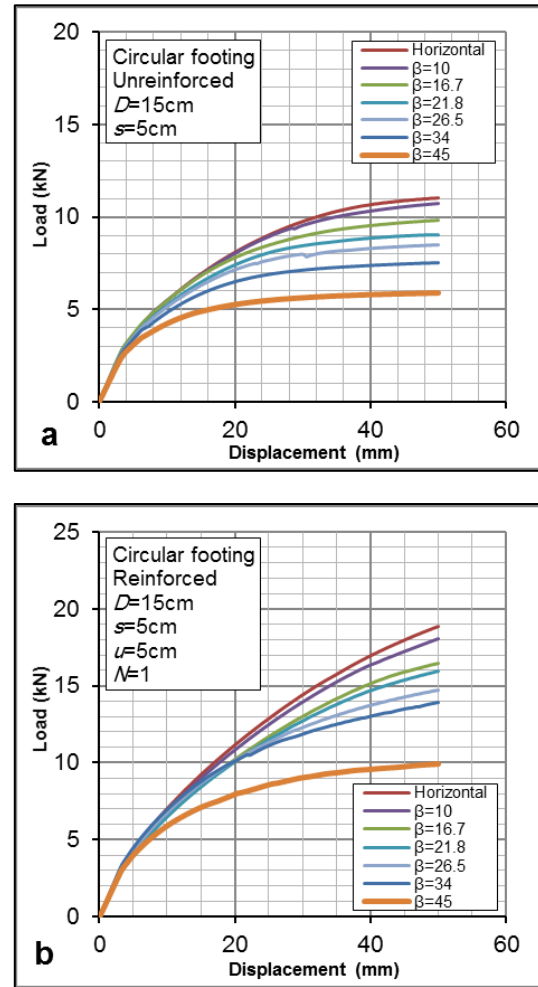
Fig. 14. Load-displacement curves for various slope angles. a) Unreinforced slope, b) Reinforced slope.

7.3 Effect of Ring Ratio

As mentioned before, the study of [3] has indicated that if the ring ratio (the proportion of inner to outer diameter of the ring footing) is less than 0.4, the bearing capacity over horizontal ground is almost the same as that

of a comparable circular footing. In order to explore this phenomenon for sand slopes, 8 models were defined with Din/Dout ranging between 0 (circular footing), and 0.67 (narrow ring footing) for both unreinforced and reinforced cases. The load bearing capacities of these models were computed and plotted versus Din/Dout (Fig17).
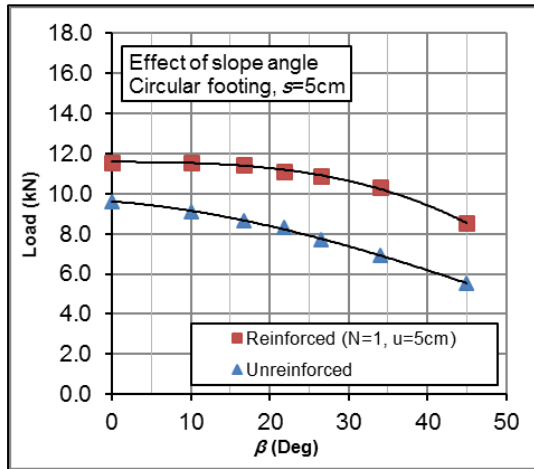

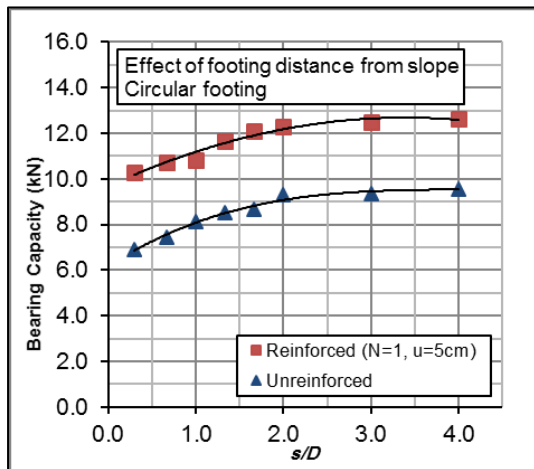**Fig. 15.** Effect of slope angle on ultimate bearing capacity

Fig. 16. The effect of distance of the footing from slope crest on ultimate bearing capacity.

It can be observed that for the ring footings with Din/Dout<0.4, the tolerated load is almost equal for both unreinforced and reinforced cases. It means that the bearing capacity of such ring footings is about equal to that of a comparable circular footing,

contemplating the other parameters equally. For narrower ring footings, bearing capacity reduces significantly to the extent that the bearing capacity of a ring footing with Din/Dout=0.6 is about 40% less than a circular footing having the similar outer diameter.

A practical advantage of the above finding is economic efficiency. From the standpoint of just bearing capacity, if a ring footing with Din/Dout<0.4 is applied instead of a circular one, the cost of materials is considerably reduced but the same bearing capacity will be achieved.
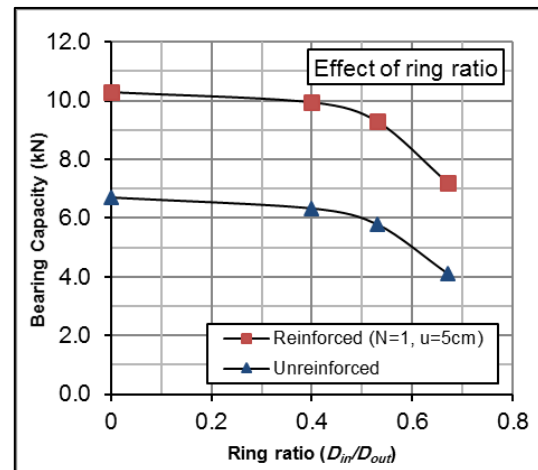

Fig. 17. The effect of ring ratio on ultimate bearing capacity.

8. Conclusions

The bearing capacity of circular and ring footings located near unreinforced and geogrid reinforced sand slopes was examined using laboratory tests and numerical simulations. The effects of geometrical parameters of reinforcement layers were investigated, On the basis of the results, if the geogrid layers are properly implemented, bearing capacity would significantly ameliorated.

It is noteworthy to mention that the study has been conducted small-scale. For field applications, real-scale simulations should be analyzed to acquire the most accurate results for each particular case.

For future studies, alternate reinforcement methods can be explored. Large-scale investigations are preferred due to the particle size effects [15], if possible economically. Moreover, seismic behavior of footings resting on reinforced slopes can be studied based on the studies conducted utilizing shaking table tests [16].

REFERENCES

[1] Binquet, J., Lee, K.L., (1975). Bearing capacity tests on reinforced earth slabs. Journal of Geotechnical Engineering, 121 (12), 1241-1255.

[2] Guido, V.A., Biesiadecki, G.L., Sullivan, M.J. (1985). Bearing capacity of geotextile reinforced foundation. Proceedings of the 11th International Conference on Soil Mechanics and Foundation of Engineers, San Francisco, CA, 1777–1780.

[3] Boushehrian, J. H., Hataf, N., (2003). Experimental and numerical investigation of the bearing capacity of model circular and ring footings on reinforced sand. Geotextiles and Geomembranes, 21, 241-256.

[4] Lee, K. M., Manjunath, V. R., (2000). Experimental and numerical studies of geosynthetic-reinforced sand slopes loaded with a footing. Canadian Geotechnical Journal, 37, 828–842.

[5] Yoo, C., (2001). Laboratory investigation of bearing capacity behavior of strip footing on geogrid-reinforced sand slope. Geotextiles and Geomembranes, 19, 279–298.

[6] Alamshahi, S., Hataf, N., (2009). Bearing capacity of strip footings on sand slopes reinforced with geogrid and grid-anchor. Geotextiles and Geomembranes, 27, 217-226.

[7] Mehrjardi, G. T., Ghanbari, A., Mehdizadeh, H. (2016). Experimental study on the behaviour of geogrid-reinforced slopes with respect to aggregate size. Geotextiles and Geomembranes, 44(6), 862-871.

[8] Hataf, N., Razavi, M. R., (2003). Behavior of ring footing on sand. Iranian Journal of Science and Technology, Transaction B, 27, 47–56.

[9] Mansur, C. L., Kaufman. J. M., (1956). Pile Tests, Low-Sill Structure, Old River, Louisiana. Journal of Soil Mechanics and Foundation Division, ASCE, 82(SM5), 1-33.

[10] Omar, M.T., Das, B. M., Puri, V. K., Yen, S.C., (1993). Ultimate bearing capacity of shallow foundations on sand with geogrid reinforcement. Canadian Geotechnical Journal, 30, 545–549.

[11] Adams, M.T., Collin, J.G., (1997). Large model spread footing load tests on geosynthetic reinforced soil foundation. Journal of Geotechnical Engineering, 123 (1), 66-72.

[12] Akinmusuru, J.O., Akinboladeh, J.A., 1981. Stability of loaded footings on reinforced soil. Journal of Geotechnical Engineering, 107 (6), 819-827.

[13] Das, B.M., Shin, E.C., Omar, M.T., (1994). The bearing capacity of surface strip foundations on geogrid-reinforced sand and clay - a comparative study. Geotechnical and Geological Engineering, 12 (1), 1–14.

[14] El Sawwaf, M. A., (2007). Behavior of strip footing on geogrid-reinforced sand over a soft clay slope. Geotextiles and Geomembranes, 25 (1), 50-60.

[15] Wang, J., Liu, F. Y., Wang, P., Cai, Y. Q. (2016). Particle size effects on coarse soil-geogrid interface response in cyclic and post-cyclic direct shear tests. Geotextiles and Geomembranes, 44(6), 854-861.

[16] Srilatha, N., Latha, G. M., Puttappa, C. (2013). Effect of frequency on seismic response of reinforced soil slopes in shaking table tests. Geotextiles and Geomembranes, 36, 27-32.